# Design and Manufacturing of the Steering System in the KMHE V1.0 Prototype Vehicle

Aydil Hijerah Harahap<sup>1</sup>, Budi Istana<sup>1\*</sup>, Sunaryo<sup>1</sup>
\*Email corresponding author: budiistana@umri.ac.id

<sup>1</sup>Department of Mechanical Engineering, Universitas Muhammadiyah Riau, Pekanbaru, 28292, Indonesia

Article history: Received: 25 Juli 2025 | Revised: 7 Septemer 2025 | Accepted: 15 Septemer 2025

Abstract. Energy-efficient prototype vehicles must combine ultra-low mass with precise, reliable steering. This work reports the design, simulation, fabrication, and testing of a lightweight rack-and-pinion steering system for a single-seat KMHE prototype. Candidate mechanisms were screened for precision, packaging, and mass; the selected layout was modeled in CAD and verified by linear static FEA with documented loading, boundary conditions, and mesh convergence. The assembled system weighs 3.74 kg, delivers an average steering ratio of 12:1, and requires 2.8 Nm steering torque under static conditions—within ergonomic guidelines. Although the measured turning radius was 6.3 m versus the 2.5 m target, analysis attributes the gap primarily to limited achievable inner-wheel angle and non-ideal Ackermann geometry, compounded by packaging stops. Peak stresses were very low (e.g., local contact pressure  $\approx 0.396$  MPa; normal/shear components  $\approx 0.07$  MPa), far below the 275 MPa yield of SUS201, with maximum displacement  $\approx 1.3 \times 10^{-5}$  mm, confirming high stiffness. The study provides a validated, lightweight steering architecture and identifies clear remedies—longer rack stroke and/or shorter steering-arm radius, corrected tie-rod pivot placement, and minor clearance revisions—to approach the target radius in the next iteration.

**Keywords -** KMHE, steering system design, prototype vehicle, rack-and-pinion mechanism, finite element analysis (FEA)

## Introduction

The steering system plays a central role in prototype vehicles, particularly those designed for competitions such as the Energy-Efficient Car Contest (Kontes Mobil Hemat Energi—KMHE). This national event challenges university students across Indonesia to design ultra-efficient vehicles that are not only energy-saving but also capable of maneuvering optimally through narrow and technical tracks. In this context, the steering system becomes one of the most vital components affecting the overall vehicle performance in terms of agility, comfort, and safety [1], [2].

One of the crucial aspects in steering system design is weight. The steering assembly falls under the category of unsprung mass, which directly affects energy consumption and vehicle stability. An increase in this mass raises wheel inertia forces, thereby reducing overall energy efficiency [2], [3], [4], [5]. For this reason, selecting lightweight materials such as aluminum alloys and adopting simulation-based structural design approaches are essential to minimize weight without compromising mechanical strength [6].

The limited space available at the front section of the prototype also poses a challenge in designing the steering system. The system must be as compact as possible so as not to interfere with other components such as the pedals, braking system, and driver's legroom. Proper and efficient placement is critical to ensure all systems function synergistically and comply with KMHE's technical regulations regarding driver positioning and cockpit safety [7] [8].

In addition to weight and spatial constraints, mechanical reliability is another key consideration. The steering system must withstand repeated steering loads and vibrations from the track surface during operation. Techniques such as topology optimization and finite element analysis (FEA) can ensure the stiffness and durability of components like knuckles and steering linkages, without adding excessive mass [9] [10].

Adequate structural strength will prevent excessive deformation that may impair vehicle maneuverability. Precision in steering geometry also determines the quality of maneuvering on the competition track [11]. The application of the Ackermann steering principle is essential in managing the angle difference between the left and right wheels when turning, thus minimizing tire slip and achieving a smaller turning radius. For the V 1.0 prototype, the target turning radius is approximately 2.5 meters, allowing it to navigate the sharp curves of the KMHE circuit [12].

Ergonomic aspects in steering design are equally important. The system must consider the driver's anthropometric dimensions to ensure comfort, effective control, and reduced muscular fatigue during driving. Previous studies on driver posture in prototype vehicles emphasize the importance of adjustable steering position, pedal reach, and seat inclination in minimizing the risk of musculoskeletal disorders, employing ergonomic assessment methods such as RULA [13].

Harahap, A. H., Istana, B & Sunaryo, Design and Manufacturing of the Steering System in the KMHE V1.0 Prototype Vehicle, R.E.M. (Rekayasa Energi Manufaktur) Jurnal, vol. 10, no. 2, pp. 115-122, 2025.

Considering all these factors including weight, dimensions, structural strength, geometry, and ergonomics this study aims to develop an optimized steering system for the V 1.0 prototype vehicle. The system is expected not only to enhance energy efficiency but also to provide excellent maneuvering performance, along with driver comfort and safety throughout the competition. This integrated design approach aligns with best practices adopted in the development of competition vehicles such as those in Formula SAE [14].

## **METHOD**

#### **Design Methodology**

This study adopted a quantitative experimental approach to design the steering system of the KMHE V 1.0 prototype vehicle. Several alternatives were first evaluated, including the bicycle-type mechanism, cable-pulley system, rack-and-pinion mechanism, four-bar linkage, and push-pull rod system. Each was assessed in terms of motion precision, mechanical reliability, transmission efficiency, and compatibility with the vehicle's limited space and lightweight requirements [15], [16].

The rack-and-pinion mechanism was selected as the most suitable solution, offering directional precision, stable response, and ease of integration with lightweight linkages [16], [17]. A CAD-based modeling process was then carried out to determine layout, dimensions, and motion compatibility (Figure 1).

Key design parameters were calculated as follows:

Steering Ratio (SR):

Steering Ratio (SR): 
$$SR = \frac{\theta_{SW}}{\theta_{fW}}$$
 (1)

where  $\theta_{sw}$  is the steering wheel rotation angle (°) and  $\theta_{fw}$  is the average front wheel turning angle (°).

Turning Radius (R):

$$R = \frac{L}{\sin\theta_i} \tag{2}$$

where L is the wheelbase (mm) and  $\theta_i$  is the inner wheel turning angle (°), consistent with Ackermann steering

These equations guided the optimization of maneuverability and stability in the prototype.

#### **Manufacturing Process**

After finalizing the design, fabrication was performed using materials selected for strength and weight efficiency. Linkages and the steering shaft were produced from 6061-T6 aluminum alloy, while the rack and pinion were fabricated from medium carbon steel (AISI 1045). The tie rod was manufactured from SUS 201 stainless steel for its balance of tensile strength and corrosion resistance as shown in Figure 1.

Fabrication steps included precision cutting, drilling, TIG welding, and assembly with strict tolerance control. Key tolerances included an installation clearance of 0.05 mm, with light interference fits for bearings and clearance fits for bracket bolts. Assembly sequence involved mounting bearings to the bracket, inserting the steering shaft, attaching tie rods, and securing the system to the chassis with M8 bolts.



Figure 1. Integration of the fabricated steering subsystem during the manufacturing process. The steering column with universal joint, intermediate shaft, center bracket, and left/right tie-rods are mounted with M8 fasteners; clearances and wheel centering were verified before static tests.

## **Initial Testing and Integration**

Static testing was conducted to verify smooth operation, proper steering angle response, and the absence of vibration or noise. Steering effort was measured using a torque wrench, determined as:

$$T = F.r \tag{3}$$

where T is the torque at the steering wheel (Nm), F is the tangential force applied at the rim (N), and r is the steering wheel radius (m).

Integration into the chassis was then performed, ensuring steering axis alignment, Ackermann geometry, and driver ergonomics (Figure 2).

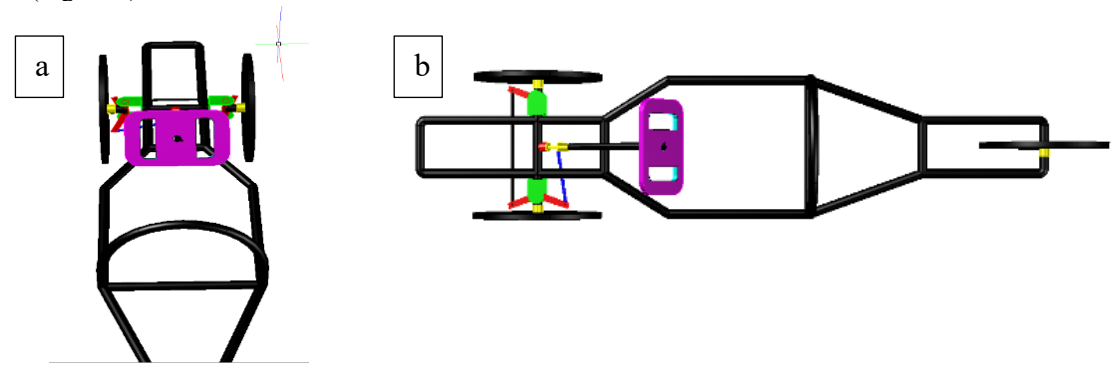


Figure 2. KMHE V1.0 chassis showing steering integration: (a) front view and (b) top view

## Structural Analysis (FEA Setup)

Finite Element Analysis (FEA) was performed to validate the structural performance of critical components, particularly the tie rod. The applied lateral force  $F_L$  was estimated as:

$$F_L = 1.5 \cdot \frac{W}{n} \tag{4}$$

where W is the vehicle weight (N) and n is the number of front wheels. The factor of 1.5 accounts for dynamic loading during cornering.

Material properties of SUS 201 stainless steel were used in the model (Elastic modulus E = 200 GPa, yield strength  $\sigma_v = 275$  MPa, Poisson's ratio v = 0.3).

Displacement was computed through numerical solvers in the CAD-FEA environment, ensuring results were compared against yield limits to assess safety margins.

## RESULT AND DISCUSSION

## A. Steering System Performance

## 1. Total Weight of the Steering System

The total weight of the steering system is a crucial parameter that affects vehicle efficiency, particularly because it contributes to the unsprung mass. Based on indivi

dual component measurements, the total weight of the steering system is as follows:

Component	Weight (kg)	
Steering shaft	2.9	
Short tie rod	0.14	
Long tie rod	0.278	
Pinion	0.0024	
Bracket	0.42	
Total	3.74 kg	

Table 1. Total Weight of the Steering System

With a total weight of 3.74 kg, the system remains lightweight for a single-seater prototype vehicle. This lightweight design is achieved through the selection of materials such as 6061-T6 aluminum alloy and efficient structural design. As supported by previous studies, choosing lightweight yet strong materials is critical for energy-

efficient vehicles. This weight is still within reasonable limits and does not significantly affect the vehicle's overall weight distribution.

## 2. Turning Radius

The turning radius is a crucial parameter for assessing vehicle maneuverability, especially on the narrow and winding circuits typical of KMHE competitions. Field testing with the steering wheel fully turned revealed a turning radius of 6.3 meters, which exceeds the original design target of approximately 2.5 meters. This discrepancy is likely due to geometric constraints such as the wheelbase length and steering angle limitations of the front wheels [15].

The measured turning radius (6.3 m) indicates an effective inner wheel angle of only ~17.6°, whereas the 2.5 m design target requires ~49.5° for L=1.9 m (R=L/sin $\theta_i$ ). The shortfall arises primarily from steering-lock limitations (rack stroke and knuckle steering-arm geometry), compounded by non-Ackermann outer-wheel behavior (outer angle ~20° vs ~41.8° ideal for L=0.263), and minor tyre/body interferences at full lock. As remedies, we will (i) increase achievable lock via a longer-stroke rack and/or a shorter steering-arm radius, (ii) reposition rack and tie-rod pivots to recover Ackermann, (iii) clear mechanical stops and wheel-arch interferences, and (iv) consider a modest wheelbase reduction in the next iteration to relax the required steering angles.

#### 3. Steering Ratio

The steering ratio is defined as the ratio between the angle of rotation of the steering wheel and the turning angle of the front wheels. It serves as a measure of the system's responsiveness to driver input. The measured values during testing were as follows in the Table 2.

ParameterValueSteering wheel rotation±300°Inner wheel turning angle30°Outer wheel turning angle20°Average Steering Ratio12:1

Table 2. Steering Ratio

The resulting average steering ratio is approximately 12:1, calculated as:

$$Steering \ Ratio = \frac{Steering \ Wheel \ Rotation}{Average \ Wheel \ Turning \ Angle}$$
 (5)

This 12:1 ratio provides an appropriate balance for a lightweight prototype, offering responsive yet stable handling. A lower ratio would increase sensitivity but could lead to oversteer, while a higher ratio might reduce maneuverability [16]. A lower ratio would increase sensitivity but could lead to oversteer, while a higher ratio might reduce maneuverability.

## 4. Steering Effort

Steering effort, or the torque required to turn the steering wheel, directly affects driver comfort. Based on measurements using a torque wrench, the steering effort under static (heaviest) conditions is 2.8 Nm.

The measured torque of 2.8 Nm falls comfortably within the optimal range for manual steering systems, which typically lies between 2 and 5 Nm [17]. This ensures ease of operation without inducing fatigue, even during static or low-speed maneuvers.

## B. Structural Analysis Using FEA

A structural analysis of the steering system was conducted using Finite Element Analysis (FEA) to determine stress distribution, strain, contact pressure, and displacement when the wheels are fully turned. The primary focus of this analysis is the tie rod, a critical component that transmits lateral forces from the wheels to the steering mechanism.

The tie-rod was analyzed in a linear static study with SUS 201 stainless steel (E=200 GPa, v=0.30,  $\sigma_y$ =275 MPa). Each rod-end eye was constrained using a remote displacement at its center with translations fixed ( $U_x$ ,  $U_y$ ,  $U_z$  = 0) and rotations free, representing spherical joints. The lateral cornering load was modeled as a remote force  $F_L$ =4414.5 N applied at the knuckle-side eye and transferred to the eye surface via rigid coupling; the rack-side eye provided the reaction. The geometry was simplified as a single solid body (threads removed) and solved with curvature-based second-order tetrahedral elements (global size  $\approx$  2.5 mm, locally 1.0 mm at fillets/bores, growth

1.3), yielding  $\approx$  79k elements and  $\approx$  145k nodes. A mesh-refinement study showed < 2% change in peak von Mises between 1.5 mm and 1.0 mm local sizes, indicating mesh-independent results. The maximum equivalent stress was < 0.5 MPa, with component values  $\sigma_{XX}\approx$ 0.070 MPa and local contact pressure at the eye  $p_Z\approx$ 0.396 MPa, all far below  $\sigma_y$ . A hand calculation for axial stress  $\sigma$ =F/A = 4414.5/11000 = 0.401 MPa matches the simulated local pressure ( $\approx$  0.396 MPa), providing an independent validation of the loading and constraint representation.

#### C. FEA Simulation Results

The FEA simulation was conducted using CAD modeling software with structural solvers to generate stress, strain, and displacement distributions for the steering system.

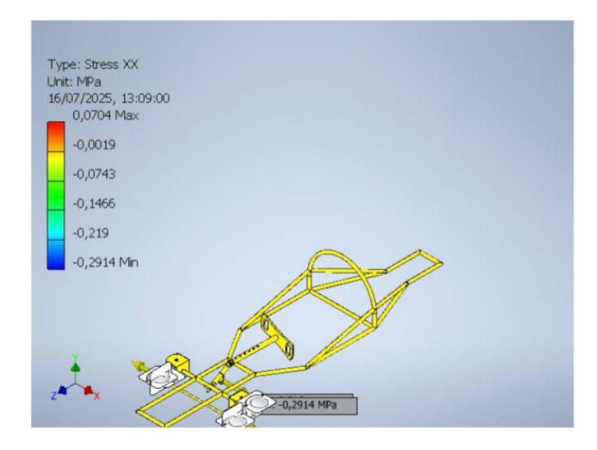


Figure 3. FEA Result: Stress Distribution in the XX Axis of the Tie Rod

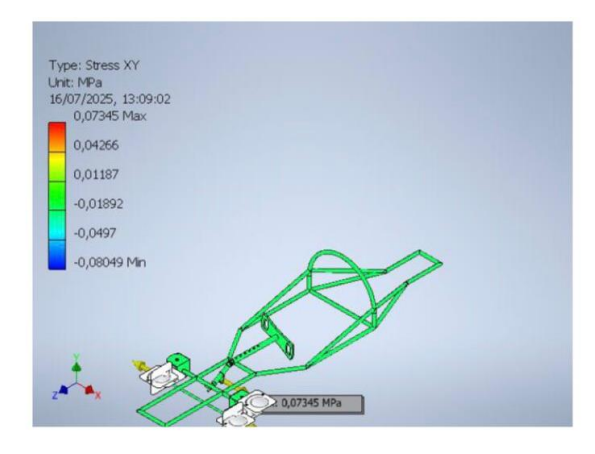


Figure 4. FEA Result: Shear Stress Distribution in the XY Axis of the Tie Rod

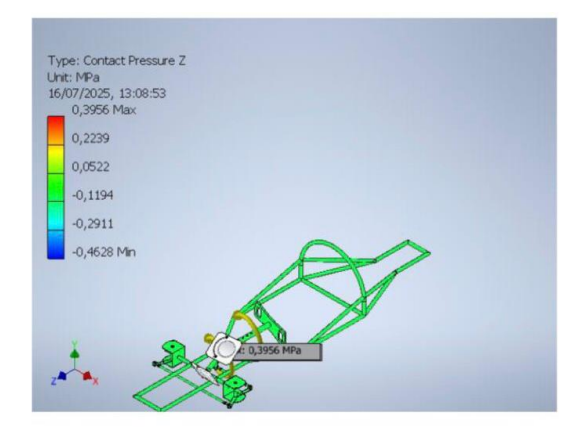


Figure 5. FEA Result: Contact Pressure Distribution in the Z Axis

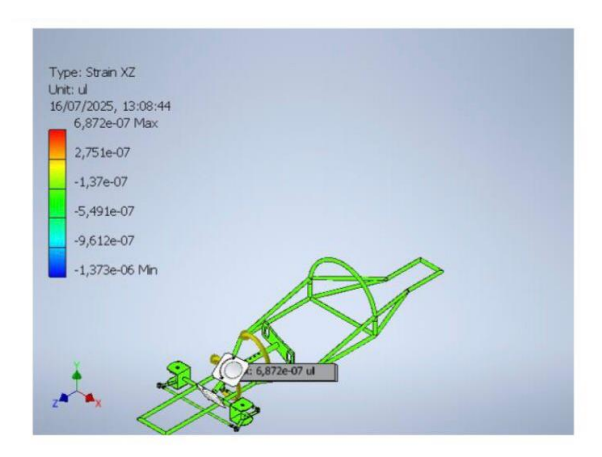
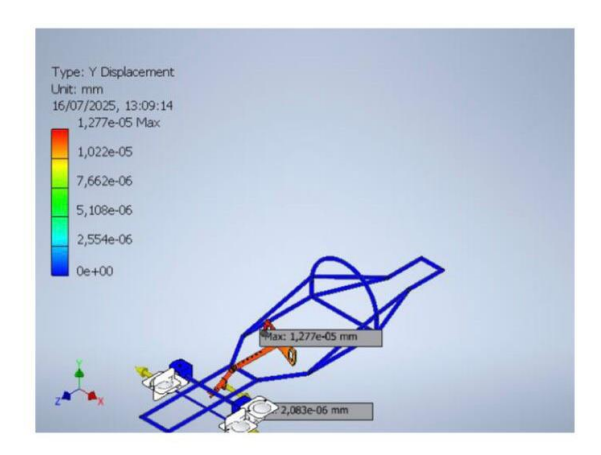


Figure 6. FEA Result: Strain Distribution in the XZ Axis



**Figure 7.** FEA Result: Displacement in the Y Axis

Type of Analysis	Max Value	Min Value
Stress XX	0.0704 MPa	-0.2914 MPa
Shear Stress XY	0.07345 MPa	-0.08049 MPa
Contact Pressure Z	0.3956 MPa	-0.4628 MPa
Strain XZ	6.872e <sup>-07</sup> με (elastic)	-1.373e-06 με (elastic)
Y Displacement	1.277e-05 mm	0 mm

Table 3. FEA Results Summary

The simulation results show that maximum stress occurs at the tie rod joint area, as shown in Figure 5, with the highest recorded value being 0.3956 MPa (Contact Pressure Z). This is far below the yield strength of SUS 201 stainless steel (approximately 275 MPa), indicating that the structure operates well within safe elastic limits, with no risk of permanent deformation under maximum load.

Other stress values, such as Stress XX and Shear Stress XY as shown in Figure 3 and 4 respectively, were only 0.0704 MPa and 0.07345 MPa respectively, further confirming the absence of critical stress zones in the system.

In terms of deformation, the maximum strain recorded was  $6.872 \times 10^{-7}$  (elastic) (Strain XZ) as shown in Figure 6, an extremely small value in the micro-scale, signifying that the structure remains within its elastic limit and can return to its original shape after loading. This is vital for steering systems, where dimensional stability directly affects directional accuracy.

As shown in Figure 7, the maximum displacement recorded in the vertical (Y) direction was only  $1.277 \times 10^{-5}$  mm. This minimal shift demonstrates excellent structural stiffness and the system's ability to withstand force without

significant deflection. High stiffness ensures that driver input is transmitted accurately to the wheels without play or deflection, maintaining steering stability and responsiveness even during extreme maneuvers.

Overall, the FEA simulation confirms that the steering system is optimally designed in terms of strength and stiffness. All stress and deformation values fall well below the material's safety thresholds, and the displacement remains negligible. This confirms the system's viability for use in single-seater prototype vehicles, offering reliability, directional stability, and safety under real-world operating conditions.

## **CONCLUSION**

This work demonstrates a lightweight, SolidWorks-based steering system for a KMHE single-seat prototype that is structurally robust and ergonomically usable. The assembled system mass is 3.74 kg, with an average steering ratio of 12:1 and a static steering torque of 2.8 Nm, which lies within accepted comfort ranges. Linear-static FEA (with documented loading, boundary conditions, and mesh convergence) indicates very low stresses (e.g., local contact pressure  $\approx 0.396$  MPa, normal/shear components  $\approx 0.07$  MPa) and a maximum displacement of  $\approx 1.3 \times 10^{-5}$  mm, well below the SUS201 yield limit, confirming high stiffness and ample safety margin.

The measured turning radius (6.3 m) exceeded the 2.5 m target. Analysis attributes this mainly to limited achievable inner-wheel angle and non-ideal Ackermann behavior, compounded by packaging stops. The next iteration will therefore (i) increase steering lock via a longer-stroke rack and/or shorter steering-arm radius, (ii) reposition rack and tie-rod pivots to recover Ackermann geometry, and (iii) remove interferences at full lock; a modest wheelbase reduction will also be evaluated to relax angle requirements.

Overall, the study provides a validated steering architecture, a transparent simulation setup, and clear, actionable design changes to close the gap to the target radius. Future work will include on-track dynamic testing (transient steering effort, compliance, and tire scrub) to complement the static validations reported here.

# ACKNOWLEDGEMENT

The authors would like to express their sincere gratitude to the Mechanical Engineering Laboratory, Universitas Muhammadiyah Riau for providing the facilities and support throughout the research. Lastly, the authors appreciate the contributions of all colleagues and team members who assisted in data collection and analysis.

# REFERENCES

- [1] Kemendikbudristek, "Pedoman Kontes Mobil Hemat Energi (KMHE) Perguruan Tinggi 2024," pp. 1–41, 2024.
- [2] W. Wang, J. Xi, C. Liu, and X. Li, "Human-Centered Feed-Forward Control of a Vehicle Steering System Based on a Driver's Path-Following Characteristics," *IEEE Transactions on Intelligent Transportation Systems*, vol. 18, no. 6, pp. 1440–1453, 2017, doi: 10.1109/TITS.2016.2606347.
- [3] Y. H. Kang, D. C. Pang, and Y. C. Zeng, "Optimal Dimensional Synthesis of Ackermann Steering Mechanisms for Three-Axle, Six-Wheeled Vehicles," *Applied Sciences (Switzerland)*, vol. 15, no. 2, 2025, doi: 10.3390/app15020800.
- [4] X. CHEN, J. YIN, W. WANG, L. WU, and F. TANG, "Approaches to diminish large unsprung mass negative effects of wheel side drive electric vehicles," *Journal of Advanced Mechanical Design, Systems, and Manufacturing*, vol. 10, no. 4, pp. JAMDSM0064–JAMDSM0064, 2016, doi: 10.1299/jamdsm.2016jamdsm0064.
- [5] M. C. Liu, C. N. Zhang, and Z. F. Wang, "Research on the Influence of Unsprung Mass on Vehicle Handling Stability," *Adv Mat Res*, vol. 562–564, pp. 816–820, Aug. 2012, doi: 10.4028/www.scientific.net/AMR.562-564.816.
- [6] S. A. N. Samin, S. Hossen, K. M. M. Rahman, and U. Gosh, "Lightweighting of a Vehicle Steering Uprights via Structural-Based Design and FEA Analysis," *Engineering Perspective*, vol. 4, no. 4, pp. 157–170, 2024, doi: 10.29228/eng.pers.78029.
- [7] C. Santana, L. Reyes-Osorio, J. Orona-Hinojos, L. Huerta, A. Rios, and P. Zambrano-Robledo, "Numerical Study of Reinforced Aluminum Composites for Steering Knuckles in Last-Mile Electric Vehicles," *World Electric Vehicle Journal*, vol. 15, no. 3, 2024, doi: 10.3390/wevj15030109.
- [8] A. Hasan, C. Lu, and W. Liu, "Lightweight Design and Analysis of Steering Knuckle of Formula Student Car Using Topology Optimization Method," *World Electric Vehicle Journal*, vol. 14, no. 9, 2023, doi: 10.3390/wevj14090233.
- [9] W. Zhang and J. Xu, "Advanced lightweight materials for Automobiles: A review," *Mater Des*, vol. 221, p. 110994, 2022, doi: 10.1016/j.matdes.2022.110994.

- [10] X. Zhang, B. Xie, Y. Yang, Y. Liu, and P. Jiang, "Research on Running Performance Optimization of Four-Wheel-Driving Ackerman Chassis by the Combining Method of Quantitative Experiment with Dynamic Simulation," *Machines*, vol. 12, no. 3, 2024, doi: 10.3390/machines12030198.
- [11] K. Polat, M. M. Topaç, and U. Çoban, "Effect of Design Parameters on Buckling Tendency of an Eccentric Drag Link Used in a Truck Steering Linkage: A DoE/RSM-Based Design Optimisation Study," *International Journal of Automotive Science and Technology*, vol. 8, no. 3, pp. 387–396, 2024, doi: 10.30939/ijastech..1484736.
- [12] V. Vyas and S. S. Shetiya, "Intelligent Electric Power Steering: Artificial Intelligence Integration Enhances Vehicle Safety and Performance," 2024.
- [13] T. Report, "Development of Column Type Electric Power Steering with Improved Level of Comfort," no. 1021, pp. 54–58, 2025.
- [14] R. R. Shamshiri *et al.*, "Online path tracking with an integrated H∞ robust adaptive controller for a double-Ackermann steering robot for orchard waypoint navigation," *Int J Intell Robot Appl*, vol. 9, no. 1, pp. 257–277, 2025, doi: 10.1007/s41315-024-00379-2.
- [15] G. Chandrashekar, M. Saikrishna, and P. Gajanan, "Study on Influence of Wheel Alignment Parameter'S for Ev Go-Kart Performance," *International Research Journal of Modernization in Engineering Technology and Science*, no. 03, pp. 1530–1535, 2024, doi: 10.56726/irjmets50255.
- [16] B. Arensen, "Design and Analysis of the Front Suspension Geometry and Steering System for a Solar Electric Vehicle," 2014.
- [17] O. M. Gul, "Energy-Aware 3D Path Planning by Autonomous Ground Vehicle in Wireless Sensor Networks," *World Electric Vehicle Journal*, vol. 15, no. 9, pp. 1–19, 2024, doi: 10.3390/wevj15090383.